Dynamics of a Massive Piston in an Ideal Gas: Oscillatory Motion and Approach to Equilibrium

N. Chernov[1,3] **and J. L. Lebowitz**[2,3]

We study numerically and theoretically (on a heuristic level) the time evolution of a gas confined to a cube of size L^3 divided into two parts by a piston with mass $M_L \sim L^2$ which can only move in the *x*-direction. Starting with a uniform "double-peaked" (non Maxwellian) distribution of the gas and a stationary piston, we find that (a) after an initial quiescent period the system becomes unstable and the piston performs a damped oscillatory motion, and (b) there is a thermalization of the system leading to a Maxwellian distribution of the gas velocities. The time of the onset of the instability appears to grow like $L \log L$ while the relaxation time to the Maxwellian grows like $L^{7/2}$.

1. INTRODUCTION

The time evolution of a gas filled container divided by a massive piston is an old problem which has attracted much attention recently from both a conceptual and computational point of view.[1–3] While we do not believe that there is any "paradox" associated with this problem, the basic mechanism of energy transport across the piston from the hot side to the cold side which are at equal pressure but different temperatures, was already described for an idealized version, by one of us in 1959,[4] many intriguing questions remain. Not surprisingly the microscopic motion of

---

[1] Department of Mathematics, University of Alabama at Birmingham, Birmingham, Alabama 35294; e-mail: chernov@math.uab.edu
[2] Department of Mathematics, Rutgers University, New Jersey 08854.
[3] Current address: Institute for Advanced Study, Princeton, New Jersey 08540.

the piston, and thus the time evolution of the system from an initial, far from equilibrium state, to the final true equilibrium state is not easy to compute analytically or even numerically for large systems.[3] It is therefore interesting to consider the greatly simplified case when the gas particles only interact via collisions with the massive piston.[4-6] This serves, among other things, as a model for the approach to equilibrium in such a "weakly" interacting macroscopic system.

Here we carry out studies on this system under the "simplest" initial conditions. The positions and velocities of gas particles of unit mass, in an insulated box of size L^3, are picked, at $t = 0$, from a Poisson process with some density function, i.e., they are assumed to be independent random variables with a given double peaked velocity distribution $p(v) = p(-v)$ (see (2.4)) and a constant spatial density throughout the box. The piston, which acts as a single particle with area L^2 and mass $M_L \sim L^2$, is then released at the position $X(0) = L/2$ with zero velocity $V(0) = 0$.

It might be thought that the random fluctuations of the piston's velocity due to the initial randomness in the positions and velocities of the gas particles will be relatively small when L is large (the number of gas particles growing like L^3) and vanish in an appropriate hydrodynamic scaling limit (as $L \to \infty$) of time, space and piston mass. In fact, some rigorous results in this direction were obtained in refs. 7 and 8 for a class of initial conditions more general than those considered here. It is proven in those papers that for those initial distributions the dynamics of the piston, in the hydrodynamic scaling limit, is governed by deterministic equations for as long as no particle collides with the piston more than twice. After that period, however, we could not control the random fluctuations in the particle configuration anymore. It is clear, though, that for an initial state which is spatially uniform and has the same velocity distribution on both sides of the piston, the deterministic macroscopic evolution would predict that the position of the piston remains stationary forever. On the other hand, when the initial velocity distribution of the particles is not Maxwellian, the system is not at thermal equilibrium, and we expect it to somehow evolve toward equilibrium for almost any initial configuration (with respect to the Liouville measure on the energy surface). This is indeed what we found for every initial distribution. The path to the Maxwellin taken by the system turned out however to be quite sensitive to the initial distribution.

Here we present the results of detailed numerical simulations for one particular initial density $p(v)$ that vanishes unless $0.5 \leqslant |v| \leqslant 1$. We found that the quiescent state becomes unstable after a few (5–10) recollisions of each gas particle with the piston. The system then develops large (on a macroscopic scale) oscillatory motions which last for a long time. They

look like smooth harmonic oscillations with an (almost) constant amplitude and piston speed comparable to that of the gas particles. Eventually, though, the oscillations dampen and vanish, and the system approaches a stable equilibrium state with constant gas density and Maxwellian velocity distribution.[4]

Our main conclusions from the numerical investigations, which we also "derive" heuristically, is that (1) while the dynamics are non chaotic in the technical sense of there being no positive Lyapunov exponents, there are for typical initial conditions[5] enough interactions to bring the system to equilibrium along "interesting" nontrivial pathways, and (2) that the time of onset of the instability grows with L as $L \log L$. This means that even on the hydrodynamical scale $\tau = t/L$, the deterministic behavior in which nothing happens on the spatial scale, $y = x/L$, would remain valid when $L \to \infty$. In terms of τ however this onset time grows only like $\log L$ so that in "practice" this behavior extends to macroscopic systems. We believe that this instability is related to the fact that the deterministic solutions are unstable for the kind of $p(v)$ we consider here. For other initial $p(v)$, for which the deterministic solution is stable, we do not get such large oscillations but, as expected, we still get an approach to Maxwellian, see Section 7.

2. DESCRIPTION OF THE MODEL

Consider a cubical container $\Lambda_L = [0, L] \times [0, L] \times [0, L]$ filled with an ideal gas consisting of N particles. The container is divided into two parts by a wall (piston) orthogonal to the x axis. At time $t = 0$ the wall is released and then it can move freely without friction inside Λ_L along the x-axis, under the action of elastic collisions with the gas particles, each of

---

[4] The latter is of course expected on general grounds for, as pointed out by Boltzmann: "[the Maxwell distribution] is characterized by the fact that by far the largest number of possible velocity distributions have the characteristic properties of the Maxwell distribution, and compared to these there are only a relatively small number of possible distributions that deviate significantly form Maxwell's. Whereas Zermelo says that the number of states that finally lead to the Maxwellian state is small compared to all possible states, I assert on the contrary that by far the largest number of possible states are "Maxwellian" and that the number that deviate from the Maxwellian state is vanishingly small",[9] see also ref. 10.

[5] Typical here means of probability converging to one (presumably, exponentially fast) as $N \to \infty$ with respect to the invariant Liouville measure. There are clearly some exceptional initial configurations (e.g., those with a complete symmetry about $x = L/2$ with opposite velocities) when $V(t) = 0$ at all times and so the speed of gas particles never changes. We expect (for the reasons given by Boltzman[9]) all such initial states to be unstable with respect to generic small perturbations.

which has the same fixed mass m. Since the piston's area is L^2, we assume its mass M_L to be proportional to L^2 and given by $M_L = bmL^2$ with a fixed constant $b > 0$ (we set $m = 1$ and $b = 2$ in our numerical simulations).

Since the components of the particle velocities perpendicular to the x-axis play no role in the dynamics of the piston, we may assume that each particle has only one component of velocity, v, directed along the x-axis. Hence, each gas particle can be specified by a pair (x_i, v_i), where $i = 1, ..., N$. We shall take the total number of particles N and the total kinetic energy of the system proportional to L^3; and we are interested in the behavior of the system for $L \gg 1$.

The initial configuration of gas particles and their velocities $\{(x_i, v_i)\}_{i=1}^{N}$ is selected at random with statistics given by a (two-dimensional) Poisson process on the x, v plane with a given density, $p(x, v) = L^2 p(v)$. More precisely, for any domain $D \subset [0, L] \times \mathbb{R}^1$ the number of particles in D, i.e., $N_D = \#\{i: (x_i, v_i) \in D\}$, has a Poisson distribution with parameter

$$\lambda_D = L^2 \int_D p(v) \, dx \, dv$$

That is, for each $k \geqslant 0$,

$$P(N_D = k) = \frac{\lambda_D^k}{k!} e^{-\lambda_D}$$

The numbers of particles in nonoverlapping domains are independent. The function $p(v) = p(-v)$ takes values of order one, and the factor of L^2 is simply the cross-sectional area of the container Λ_L. The piston is initially at rest at the midpoint, $X(0) = L/2$, $V(0) = 0$ and the position and velocity at time t are denoted by X, $0 \leqslant X \leqslant L$, and V.

We note that the total number of gas particles N in the container is random. So are the numbers of particles to the left and to the right of the piston, call them N_- and N_+, respectively ($N = N_- + N_+$). The initial total kinetic energy of the system, $\frac{1}{2} \sum m v_i^2$, is also a random variable. Once chosen, the values of N_-, N_+ and the total kinetic energy E of gas plus piston are (presumably, the only) integrals of motion.

The gas particles and the piston move freely (with constant velocity) between elastic collisions of particles with the piston and the walls. When a particle collides with a wall at $x = 0$ or $x = L$, its velocity simply reverses. If a particle with velocity v hits the piston whose velocity is V, then their velocities after the collision, call them v' and V', respectively, are given by

$$V' = (1 - \varepsilon) V + \varepsilon v \tag{2.1}$$

$$v' = -(1 - \varepsilon) v + (2 - \varepsilon) V \tag{2.2}$$

where

$$\varepsilon = \frac{2m}{M+m} = \left(\frac{2}{bL^2+1}\right) \tag{2.3}$$

In order to avoid recollisions of gas particles with the piston, for at least some initial period of time, we impose a velocity cutoff[6]

$$p(v) \equiv 0 \qquad \text{if} \quad |v| \geqslant v_{\max} \qquad \text{or} \quad |v| \leqslant v_{\min} \tag{2.4}$$

with some $0 < v_{\min} < v_{\max} < \infty$, cf. refs. 8 and 7. Under these conditions, there will be an initial time interval of length $O(L)$ during which each particle colliding with the piston will have to travel to the wall, bounce off it, and then travel back to the piston before it can hit it again. Therefore, during that interval, there will be no recollisions of any gas particle with the piston. We call such an interval of time the zero-recollision interval. Likewise, if the piston remains slow enough after recollisions occur, there will be another interval of time of order L during which each gas particle experiences at most one recollision with the piston. We call it the one-recollision interval.

The *hydrodynamic limit* is now obtained by rescaling space, $y = x/L$, $0 < y < 1$, and time, $\tau = t/L$. In the new space-time coordinates y, τ the zero-recollision interval and the one-recollision interval will be of order one, and we will denote them by $(0, \tau_0)$ and (τ_0, τ_1) respectively. As already mentioned, we prove in ref. 8, for a more general class of initial densities $p(x, v)$ that during the interval $(0, \tau_1)$ the functions $Y_L(\tau)$ and $W_L(\tau)$

$$Y_L(\tau) = X(\tau L)/L, \qquad W_L(\tau) = dY_L/d\tau = V(\tau L)$$

converge uniformly in probability, as $L \to \infty$, to some deterministic functions $\bar{Y}(\tau)$ and $\bar{W}(\tau)$; $\bar{W}$ satisfies a certain algebraic equation and $d\bar{Y}/d\tau = \bar{W}$. In the case considered here, when the density function $p(x, v)$ is independent of x and symmetric in v, i.e., $p(v) = p(-v)$ for all x, v, then the hydrodynamic evolution is trivial: $\bar{Y}(\tau) \equiv 0.5$ and $\bar{W}(\tau) \equiv 0$ for all $\tau > 0$. Hence, $Y_L(\tau) \to 0.5$ and $W_L(\tau) \to 0$ as $L \to \infty$, uniformly for all $\tau \in (0, \tau_1)$.

In this paper we investigate numerically what happens to $Y_L(\tau)$ and $W_L(\tau)$ beyond the interval $(0, \tau_1)$. More precisely, for how long does the stochastic trajectory $\{Y_L(\tau), W_L(\tau)\}$ remain close to the deterministic one $\{\bar{W}(\tau), \bar{Y}(\tau)\}$? And what does it look like in the long run?

---

[6] As explained in Section 7, the choice of $p(v)$ plays an important role in the later time evolution of the system.

3. NUMERICAL RESULTS

In the computer simulations described here and in Sections 4–6, we set

$$p(x, v) = p(v) = \begin{cases} 1 & \text{if} \quad 0.5 \leqslant |v| \leqslant 1 \\ 0 & \text{elsewhere} \end{cases} \tag{3.1}$$

so $v_{\min} = 0.5$ and $v_{\max} = 1$. The x and v coordinates of all the particles are then independent random variables uniformly distributed in their ranges $0 < x < L$ and $v_{\min} \leqslant |v| \leqslant v_{\max}$. Our computer program first selects N according to the Poisson law with mean L^3, and then generates all (x_i, v_i), $1 \leqslant i \leqslant N$, independently according to their uniform distributions. We used the random number generator described in ref. 11. The parameter L changed in our simulations from $L = 30$ to $L = 300$. For $L = 300$ the system contains $\approx L^3 = 27, 000, 000$ particles.

Once the initial data is generated randomly, the program computes the dynamics by using the elastic collision rules (2.1), (2.2). All calculations were performed in double precision, with coordinates and velocities of all particles stored and computed individually. We note that memory requirements alone can be enormous—the program needs over 430 Mb RAM in order to run the model with $L = 300$. Also, the task of determining which particle is to collide with the piston next is nontrivial. To avoid a long search through the entire set of N particles after each collision, we assembled a smaller group of particles located in a vicinity of the piston, where the search is performed, and updated this group periodically, as time goes on. The calculations were done in $C++$ and HPF (High Performance Fortran) on a Dell Power Edge machine with Dual 733MHz processors at the University of Alabama in Birmingham. Our code is available on the web page referred to in the next section.

Figure 1 presents a typical trajectory of the piston. Here $L = 100$. The position and time are measured in hydrodynamic variables $Y = X/L$, $0 < Y < 1$, and $\tau = t/L$.
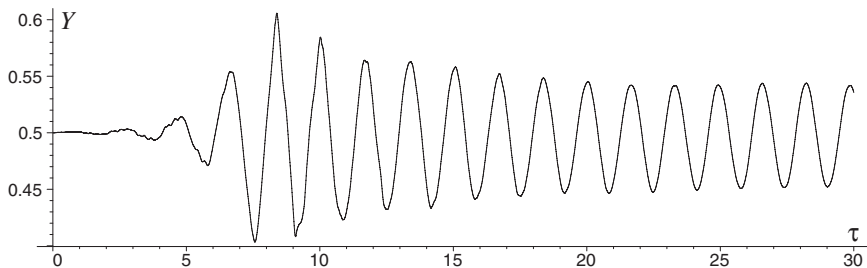

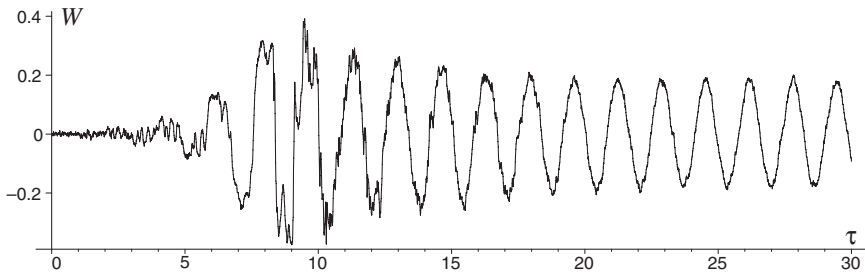Fig. 1.   The piston coordinate Y as a function of time τ. Here $L = 100$, $N_- = 500341$, $N_+ = 499888$.

Fig. 2. The piston velocity W as a function of time τ. The same run as in Fig. 1.

Initially, the piston barely moves about its equilibrium position: recall that the hydrodynamic trajectory of the piston is $\bar{Y}(\tau) \equiv 0.5$ for all $\tau > 0$ and that this holds exactly for $\tau < 2$ as $L \to \infty$.[8] Then, at times τ between 3 and 5, the random vibrations of the piston grow and become quite visible on the y-scale, but for a short while they look random. After that the piston starts travelling back and forth along the y axis, making excursions farther and farther away from the equilibrium point $y = 0.5$. Very soon, at $\tau = \tau_{max} \approx 8$, the swinging motion of the piston reaches its maximum, $(\Delta Y)_{max} = \max |Y(\tau) - 0.5| \approx 0.1$. Then the oscillations of the piston dampen in size and seem to stabilize at an amplitude $A \approx 0.04$. At the same time the trajectory of the piston smoothes out and enters an oscillatory mode with a period $\tau_{per} \approx 1.63$.

The velocity of the piston $W(\tau)$ follows a similar pattern. Its random fluctuations grow after $\tau \approx 2.5$, then it starts swinging up and down, reaches the maximum value of $W_{max} = \max |W(\tau)| \approx 0.4$ at time $\tau \approx 9.5$. After that the oscillations of $W(\tau)$ dampen and seem to stabilize.

Note that the graph of the function $Y(\tau)$ looks much smoother than that of $W(\tau)$, as would be expected from the fact that $Y(\tau)$ is the integral of $W(\tau)$. Interestingly, both functions Y and W smooth out as time goes on.
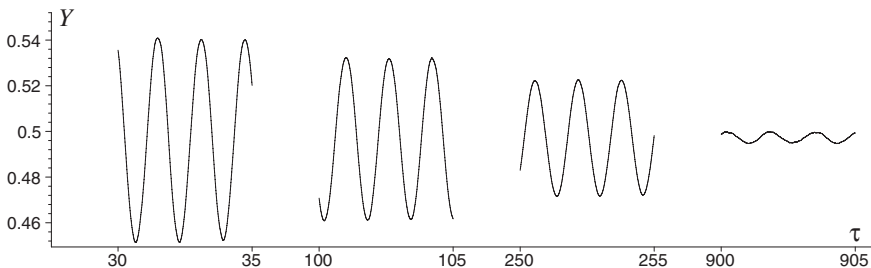

Fig. 3. The piston coordinate Y during the intervals $(30, 35)$, $(100, 105)$, $(250, 255)$, and $(900, 905)$. The same run as in Figs. 1 and 2.

This cycle of the gas motion in the container between the walls and the piston continues for a long time with the same period $\tau_{per} \simeq 1.63$, independent of L, but the amplitudes of both $Y(\tau)$ and $W(\tau)$ are slowly decreasing, see Fig. 3.

The oscillations of the piston with decaying amplitude can be described, in the interval $30 < \tau < 1000$, approximately by

$$Y_1(\tau) \simeq A e^{-\lambda(\tau-20)} \sin \omega(\tau-\alpha) \tag{3.2}$$

with $A = 0.046$ and some constant $\lambda > 0$. Correspondingly, $W_1(\tau) = dY_1/d\tau$ in the same interval $30 < \tau < 1000$ is

$$\begin{aligned}
W_1(\tau) &\simeq -\lambda Y_1 + A e^{-\lambda(\tau-20)} \omega \cos \omega(\tau-\alpha) \\
&= A e^{-\lambda(\tau-20)} [-\lambda \sin \omega(\tau-\alpha) + \omega \cos \omega(\tau-\alpha)] \\
&= A_1 e^{-\lambda(\tau-20)} \sin \omega(\tau-\beta) \tag{3.3}
\end{aligned}$$

with $A_1 = A\sqrt{\omega^2 + \lambda^2}$ and some β related to α.

To check how well our formula (3.2) agrees with the data, we computed the amplitude $A(\tau)$ as a function of time τ, by fitting a sine function $Y_0(\tau) = A \sin \omega(\tau-\alpha)$ "locally", on the interval $(\tau-5, \tau+5)$ for each τ. Figure 4 shows $A(\tau)$ on the logarithmic scale, which looks almost linear on the interval $30 < \tau < 800$. (After that, $Y(\tau)$ becomes quite unstable, with already small amplitude $A(\tau)$ decreasing abruptly, possibly due to the interference from random fluctuations, so we left that part out.)

We used the least squares fit to estimate $\lambda = 0.00264$ for the run shown on Figs. 1–4. Since λ is small, the oscillations indeed die out very slowly. The "half-life" time (the time it takes to reduce the amplitude by a factor of two) is $\tau_{1/2} = \lambda^{-1} \ln 2 \approx 263$. Note that over the time interval
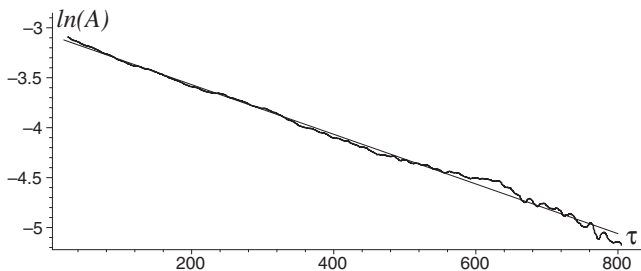

Fig. 4.   The amplitude $A(\tau)$ on the logarithmic scale: experimental curve (bold) and a linear fit (thin). The same run as the one shown in Figs. 1, 2 and 3.

Table I.   Principal Characteristics of the Piston Dynamics

L	$(\Delta Y)_{\max}$	$W_{\max}$	A	τ_{per}
30	0.114	0.40	0.042	1.70
50	0.121	0.39	0.045	1.65
80	0.105	0.37	0.042	1.65
100	0.100	0.34	0.041	1.64
120	0.122	0.39	0.041	1.62
150	0.111	0.37	0.045	1.62
200	0.102	0.37	0.037	1.62
250	0.100	0.41	0.042	1.64
300	0.122	0.42	0.045	1.65

$30 < \tau < 800$ we only observed the reduction of the amplitude by a factor of about 10, and the periodic oscillations were still visible on the plot at $\tau > 900$. Also, λ and hence $\tau_{1/2}$ depend on the system size L, see below.

4. DEPENDENCE OF THE TIME EVOLUTION ON SYSTEM SIZE

Many of the characteristics of the piston trajectory described above ($(\Delta Y)_{\max}$, $W_{\max}$, A, τ_{per}) appear to be independent of L. The following table[7] presents computed values of all these parameters for different L's.

In each case, we averaged over several experimentally generated trajectories (for $L = 250$ and 300, just one trajectory was used).

There are however other quantities such as $\tau_{\max}$, $\tau_{1/2}$, and the related λ, which depend in a systematic way on L. In particular, we estimated numerically that $\tau_{1/2} \sim L^{1.3}$, hence $\lambda \sim L^{-1.3}$, see Fig. 5. We will denote $\lambda = \lambda_L$ and discuss it further in Section 6. We also noticed that in some runs with larger L's (such as $L = 150$ and $L = 200$) the exponent λ changes with time, it is higher when $\tau < 100$ and lower when $\tau > 100$.

But most importantly, the time of the largest oscillations $\tau_{\max}$ and the related time of the onset of the instability τ_c, see below, seem to slowly grow with L, very likely as $\log L$. To understand this fact, we looked into the mechanism of the build-up of random fluctuations of the piston position and velocity, which eventually result in their large nearly harmonic oscillations. To this end we plotted the histogram of the (empirical) density of gas particles in the y, v plane at various times $0 < \tau < 30$, see samples in

---

[7] The numerical data here are given primarily for demonstrating the typical scale of oscillations. They are not meant to be estimates of physical parameters, so we do not provide error bars. For $L \leqslant 200$, where more than one experimental trajectory was generated, we have estimated that the accuracy of our numerical values in Table I is at least within 10%.
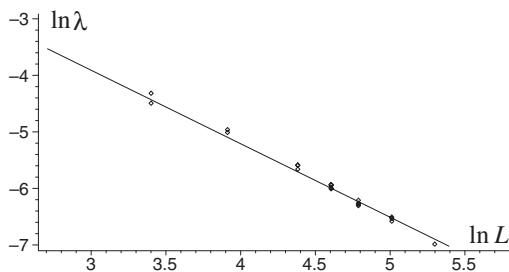
Fig. 5.   The value $\ln \lambda$ as a function of $\ln L$: experimental points and a linear fit.

Fig. 6. The initial density (at time zero) is almost uniform over the domain $0 < x < L$ and $v_{\min} \leqslant |v| \leqslant v_{\max}$ (variations in the initial configuration always exist, because it is generated randomly). Then, for $0 < \tau < 1$, the piston experiences random collisions with particles and acquires a speed of order $M_L^{-1/2} = O(1/L)$, see refs. 4, 12, and 13. These small fluctuations of the piston velocity result in changes of the velocities of the particles which
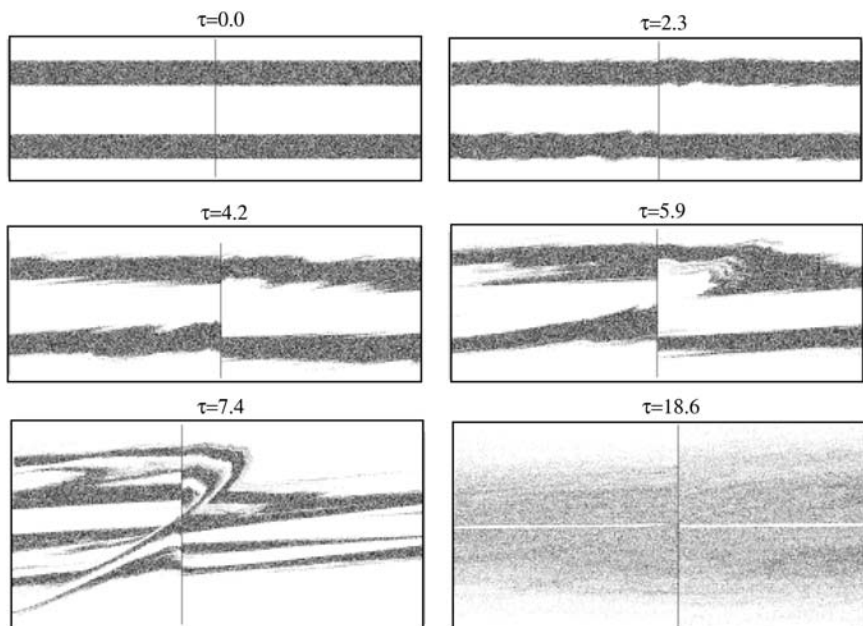

Fig. 6.   Six snapshots of the empirical gas density (in the x, v plane) at times $\tau = 0$, 2.3, 4.2, 5.9, 7.4 and 18.6.

leave the piston after collision. Thus the outgoing particles on the right hand side of the piston have velocities in the interval $(v_{\min} + 2W(\tau), v_{\max} + 2W(\tau))$ while those on the left hand side of the piston have velocities in the interval $(-v_{\min} + 2W(\tau), -v_{\max} + 2W(\tau))$. Hence, the region in the y, v plane where the density of the particles is positive is no longer a rectangle with straight sides, now its boundaries are curves whose shape nearly repeats the graph of the randomly evolving piston velocity $W(\tau)$. While the variations of $O(1/L)$ of these boundary curves may seem small, it is crucial that on opposite sides of the piston they go in opposite directions. Indeed, when $W(\tau) > 0$, then the outgoing particles on the right hand side accelerate and those on the left hand side slow down. When $W(\tau) < 0$ the opposite happens.

Next, the particles that have collided with the piston travel to the wall and come back to the piston. Now their densities are less regular than they were initially—the regions in the x, v plane where the density is positive, are curvilinear domains. When they hit the piston, they shake it back and forth more forcefully than before, because the velocities of the incoming particles on the opposite sides of the piston are now negatively correlated. When particles on the right hand side are fast, those on the left hand side are slow, and vice versa. This produces a resonance-type effect destabilizing the piston dramatically and the velocity of the piston $W(\tau)$ experiences larger fluctuations than before. The velocities of the newly outgoing particles will again go up and down in opposite direction, on a greater scale than before.

As time goes on, the above phenomenon repeats over and over, with larger and larger fluctuations of the gas and piston velocities, until the distribution of gas particles completely breaks down. At times $\tau \sim 10$, two large clusters of particles are formed, one on each side of the piston. When one cluster bombards the piston, the other moves away from it and hits the wall, then they exchange their roles. The clusters have sizes of about 0.3–0.5 in the y direction and the particle velocities range from about 0.2 to just over 1. The average velocity is about 0.5–0.6 and so the clusters hammer the piston periodically with period 1.6–2.0, which is close to the experimentally determined period of piston oscillations, see above.

Figure 6 shows six snapshots of the empirical density of gas particles taken at different times. At $\tau = 0$ the gas fills (almost uniformly) two rectangles $\{(y, v) : 0.5 < |v| < 1, 0 < y < 1\}$. At $\tau = 2.3$ one can see some ripples on the boundaries of these rectangles. At time $\tau = 4.2$ the irregularities grow and at $\tau = 5.9$ the rectangular shape is broken down. Two large clusters of particles are formed, both appear in the upper half-plane $v > 0$, i.e., at that time both clusters move to the right (one toward the piston, the other away from it). Later the density undergoes strange formations

($\tau = 7.4$) but eventually smoothes out and enters a slow process of convergence to Maxwellian ($\tau = 18.6$) described below. Note a narrow white line around $v = 0$, meaning the total lack of very slow particles at time $\tau = 18.6$.

A longer sequence of snapshots at times $0 < \tau < 30$ is posted on the web page

www.math.uab.edu/chernov/piston/pictures/piston.html

It gives a spectacular view of the entire system evolution.

The above analysis may suggest that the fluctuations of the piston velocity roughly increase by a constant factor during each time interval of length one. Indeed, initial random fluctuations $W_a \sim O(1/L)$ result in additional changes of velocities of outgoing particles by $2W_a$. When those particles come back to the piston (in time $\Delta\tau \approx 1$), they kick its velocity to the level of $2W_a$. Then the newly outgoing particles acquire an additional velocity $4W_a$, etc. Over each time interval of length one the fluctuations double in size. This is an obvious oversimplification of the real dynamics, but it leads to a reasonable conjecture

$$W_a(\tau) \approx \frac{CR^\tau}{L} \tag{4.1}$$

where $W_a(\tau)$ are typical fluctuations of the piston velocity at time τ and $C, R > 0$ are constants.

We tested the above formula numerically as follows. Let $W_c > 0$ be some preset critical value of the piston speed and $\tau_c = \inf\{\tau > 0 : |W(\tau)| \geqslant W_c\}$ the (random) time when W_c is first reached. This time plays the role of the "onset" of large fluctuations of the piston velocity. One would expect, based on (4.1) that

$$\tau_c \approx \ln(W_c L/C)/\ln R \tag{4.2}$$
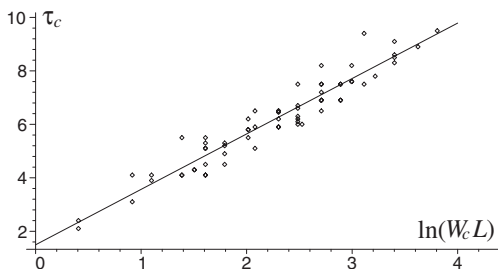
i.e., τ_c grows as $\ln L$ when L increases.

Fig. 7. The value τ_c as a function of $\ln(W_c L)$: experimental points and a linear fit.

We found τ_c experimentally for $W_c = 0.1$ and $W_c = 0.15$ and checked that (4.2) agreed well with the data, see Fig. 7. By the least squares fit we estimated $C = 0.45$ and $R = 1.6$.

5. APPROACH TO EQUILIBRIUM

We examined the convergence of the velocity distribution of gas particles to a Maxwellian. At any given time $\tau > 0$, let

$$F_\tau(u) = \#\{i : v_i < u\}/N$$

be the empirical (cumulative) distribution function of particle velocities. At equilibrium, it should be close to the normal distribution function $\Phi(x)$. As a measure of their closeness, we used the supremum of the difference

$$D_\tau = \sup_{-\infty < u < \infty} |F_\tau(u) - \Phi(u)|$$

Initially, $D_0 \approx 0.245$ for our choice of $p(v)$. One can expect that D_τ converges to 0 as τ grows when N is large. In fact, if the velocities v_i were independent and had Maxwellian distribution (which it would be in true statistical equilibrium), then D_τ would be of order $O(1/\sqrt{N})$, and the product $D_\tau \sqrt{N}$ would have a certain limit distribution, see the theory of the Kolmogorov–Smirnov statistical test.[14] In particular, it is known that for a Maxwellian the probability $P(D_\tau \sqrt{N} > 1) \approx 0.2$. Based on this, we define the time of convergence to equilibrium by

$$\tau_{eq} = \inf\{\tau > 0 : D_\tau \sqrt{N} < 1\} \tag{5.1}$$

Here the constant 1 as a critical value is chosen arbitrarily. We estimated τ_{eq} for various L's and found that $\tau_{eq} \approx aL^b$ with some constants $a, b > 0$. By a least squares fit we found $a = 0.18$ and $b = 2.47$, see Fig. 8. (Note that the accuracy of our experimental data seems to increase with L, as the points are getting closer to each other and to the fitting line for larger L's on Fig. 8.)

The plot of the product $S = D_\tau \sqrt{N}$ versus τ is given on Fig. 9 (for a particular run with $L = 40$). It shows that, after an initial sharp drop for $0 < \tau < 20$, the statistic S decreases exponentially in τ. Another commonly used statistic to measure closeness to Maxwellian is
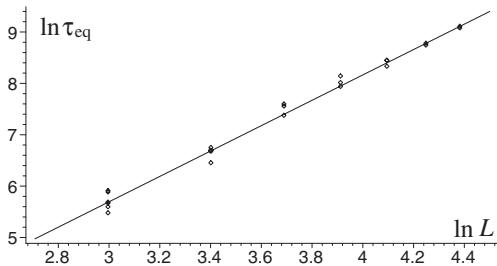
$$S' = 3 - \frac{M_4}{M_2^2}$$

Fig. 8. The value $\ln \tau_{eq}$ as a function of $\ln L$: experimental points and a linear fit.

where M_2 and M_4 are the second and the fourth sample moments of the empirical velocity distribution, respectively. Figure 9 shows that S' converges to zero in a similar manner (for the same run with $L = 40$).

Theoretical Considerations

As we noted in Section 2, the total energy E and the numbers of particles in the left and right compartments (N_- and N_+) are integrals of motion. With these quantities fixed, the model can be reduced to a billiard system in a high-dimensional polyhedron by standard techniques, as we show next.

Let $\{x_i\}$, $i = 1, \ldots, N_+$, denote the x-coordinates of the particles to the right of the piston, and $\{x_i\}$, $i = -1, \ldots, -N_-$, those to the left of it (ordered arbitrarily). Put $x_0 = X\sqrt{M}$, where X is the coordinate of the piston and M is its mass. Then the configuration space of the system (in the coordinates x_i, $-N_- \leqslant i \leqslant N_+$) is a polyhedron $Q \subset \mathbb{R}^{N+1}$ (recall that $N = N_- + N_+$) defined by inequalities

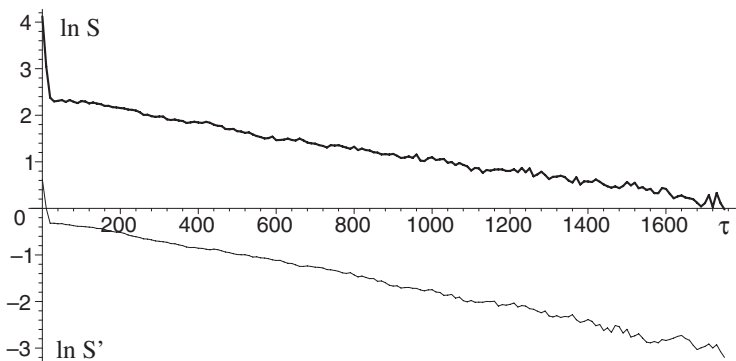$$0 \leqslant x_{-N_-}, \ldots, x_{-1} \leqslant x_0/\sqrt{M} \leqslant x_1, \ldots, x_{N_+} \leqslant L$$

Fig. 9. $\ln S$ (thick line) and $\ln S'$ (thin line) as functions of τ.

It is known that the dynamics of our mechanical system ("gas + piston") corresponds to the billiard dynamics in Q, see ref. 15. That is, the configuration point $\mathbf{q} \in Q$ moves freely and experiences specular reflections at the boundary ∂Q. The velocity vector

$$\mathbf{p} = \dot{\mathbf{q}} = \{v_{-N_-}, ..., v_{-1}, V \sqrt{M}, v_1, ..., v_{N_+}\}$$

has constant length, since $\|\mathbf{p}\|^2 = 2E = \text{const}$. Therefore, the phase space of the billiard system is $\mathcal{M} = Q \times S_\rho^N$ where S_ρ^N is the N-dimensional sphere of radius $\rho = \sqrt{2E}$.

The billiard system has a natural equilibrium state given by the Liouville measure μ on $\mathcal{M}$, which is the product of a uniform measure on the polyhedron Q and a uniform (Lebesgue) measure on the sphere S_ρ^N, i.e., $d\mu = dq\,dp$. The properties of billiard dynamics depend heavily on the curvature of the boundary ∂Q. In our case Q is a polyhedron, hence its boundary consists of flat sides with zero curvature. A prototype of such systems is billiard in a polygon. It is well known that (see, e.g., ref. 16)

Fact. For billiards in polygons and polyhedra (and hence, for our mechanical model of a piston in the ideal gas) all Lyapunov exponents vanish, and so does the Kolmogorov–Sinai entropy.

Systems with zero Lyapunov exponents and zero entropy are not regarded as chaotic, but they still may be ergodic. In fact, billiards in generic polygons *are* ergodic.[17] Moreover, for many nonergodic polygons, the phase space is foliated by invariant subsurfaces on which the dynamics is ergodic.

Even though there are no similar results, to our knowledge, for billiards in high-dimensional polyhedra, one can expect that they, too, have similar properties. That is, they are generically ergodic or become ergodic after trivial reductions. In our case, the billiard in Q is, perhaps, ergodic for typical values of M, or else the phase space is foliated by invariant submanifolds on which the dynamics is ergodic, and that those submanifolds fill $\mathcal{M}$ pretty densely. In the latter case, one would hardly distinguish experimentally between such a nonergodic system and a truly ergodic one.

Hence, we can assume that our system is ergodic or very close to ergodic in the above sense. Then almost every trajectory eventually behaves according to the invariant measure μ, independently of the initial state. In particular, for any initial gas density and velocity distribution (given by the function $p(x, v)$, see Section 2) the hydrodynamic regime for a finite L is only valid on a finite interval of time–eventually the system will relax to equilibrium. We expect in fact that in terms of the "macroscopic" variables, say, the one particle distribution function, the system will relax

to an effective equilibrium, as defined by (5.1) in terms of τ_{eq}, which is much smaller than the exponentially long time (in L) required for the ergodic theorem. So the real question is how does this time depend on L. According to our earlier discussion $\tau_c \sim \log L$ and $\tau_{eq} \sim L^{5/2}$.

At equilibrium, the distribution of coordinates x_i and velocities v_i are determined by the Liouville measure μ, which is uniform in the phase space. Physically interesting (and only observable) are its marginal measures, i.e., projections, on lower-dimensional subspaces. The marginal measures of the velocities are normal (Gaussian) for large N (as $N \to \infty$).

In particular, each individual velocity v_i converges in law to a Maxwellian (i.e., normal) distribution with zero mean and variance $2E/N = \text{const}$. The same holds for the "piston" component of the velocity, $\dot{x}_0 = V\sqrt{M}$, hence the piston velocity V will be normally distributed with zero mean and standard deviation $\text{const}/\sqrt{M} = \text{const}/L$, as $L \to \infty$. In our case V has standard deviation $\sqrt{7/24}/L \approx 0.5/L$. This conclusion agrees well with our numerical data.[8]

The equilibrium distribution of the piston coordinate X is also determined by the projection of the uniform measure dq on Q onto the x_0 axis. Before we do that, let us get rid of M in the definition of both Q and x_0. A simple change of variable $X = x_0/\sqrt{M}$ allows us to redefine Q by

$$0 \leqslant x_{-N_-}, ..., x_{-1} \leqslant X \leqslant x_1, ..., x_{N_+} \leqslant L$$

Furthermore, rescaling $Y = X/L$ and $y_i = x_i/L$ gives a new, simpler, definition of Q:

$$0 \leqslant y_{-N_-}, ..., y_{-1} \leqslant Y \leqslant y_1, ..., y_{N_+} \leqslant 1$$

"Integrating away" the variables y_i yields the following equilibrium density for Y:

$$f(Y) = cY^{N_-}(1-Y)^{N_+}$$

for $0 < Y < 1$, where c is the normalizing factor that can be computed explicitly. Put $z = (Y - 0.5)\sqrt{8K}$, then the density of z is given asymptotically

---

[8] It also allows us to estimate, in a peculiar way, the time of convergence to equilibrium, τ_{eq}, discussed earlier. Assume all the initial velocities are of order one, and note that the largest Maxwellian velocities are of order $\sqrt{N} = L^{3/2}$. Since each collision with the piston adds $O(1/L)$ to a particle's velocity, it takes $\sim L^{5/2}$ collisions to reach the maximum. An amazing agreement with the estimate $\tau_{eq} \sim L^{2.47}$ reported near Fig. 8.

by $f(z) \approx \frac{1}{\sqrt{2\pi}} e^{-z^2/2}$. Hence, Y is asymptotically gaussian with mean 0.5 and variance $(4N)^{-1} = (4L^3)^{-1}$. Therefore, in equilibrium

$$|Y - 0.5| \sim \frac{1}{2L\sqrt{L}} \sim \frac{1}{2\sqrt{N}}$$

and the probability of observing larger fluctuations is exponentially small in N. Note that fact is independent of the piston mass, as it has to be for an equilibrium (classical) system. This is consistent with our observation of the piston coordinate reaching a positive constant value, $|Y - 0.5| \approx 0.1$, during a short time interval $0 < \tau < 20$, since our initial conditions were selected according to the density function $p(x, v)$ which has probability exponentially small in N.

6. REMARKS

1. We checked the accuracy of our computer program in various ways. A simple one was based on the effect of round-offs on the energy of the system: the total energy was found to be practically constant over the whole period $0 < \tau < 1000$. A more sensitive test of the accuracy of the computations consists in using the time-reversal symmetry of the dynamics. Suppose at some time $\bar{\tau} > 0$ the velocities of all gas particles and the piston are reversed ($v_i \to -v_i$). Then the system is supposed to trace back its past trajectory and arrive to its initial state with all velocities reversed at time $2\bar{\tau}$. We verified this property numerically for various $\bar{\tau} < 50$ and always found that the system did repeat its past trajectory in the sense that the graphs of $Y(\tau)$ and $W(\tau)$ over the interval $(\bar{\tau}, 2\bar{\tau})$ looked like perfect mirror images of the corresponding graphs over the interval $(0, \bar{\tau})$. Therefore, one can assume that round off errors remain negligibly small during times $\tau < 50$. However, this accuracy test failed for larger times, $\bar{\tau} > 100$, indicating that the system then "loses memory" of its initial state due to round-offs. This does not seem to affect the overall picture, though. As yet another test, we carried out some computations with single rather than double precision, and found that the changes were little. Still, some estimates requiring long runs, such as the equilibrium time τ_{eq} on Fig. 8, might not be very accurate.

2. We tested the dependence of the piston oscillations on the b factor involved in the formula $M_L = bmL^2$. Remember that we set $b = 2$ in our main experiments. When we changed it to $b = 20$ (this made the piston 10 times heavier), then the oscillations started slightly later and their amplitude was slightly larger, but otherwise the picture was very much the

same. When we changed b to 0.2 (and this made the piston 10 times lighter), then the oscillations started at about the same time as for $b = 2$, but they dampened somewhat faster.

We also tried to change the piston mass M_L even more drastically. When we set it to L^3 (insteas of L^2), it appeared that oscillations started only after a very long initial quiescent period. But we did not examine this fact in detail, see ref. 18. On the contrary, when we set the piston mass M_L to L (instead of L^2), large oscillations started very soon, but very quickly dampened and disappeared.

3.   We note that Eq. (3.3) describes the time evolution of a damped harmonic oscillator. Accepting (3.3) over some time range, say, $\tau \in [30, 800]$ for $L = 100$, we can then look at the "inverse problem" of finding the effective spring constant and damping coefficient.

Using the original variables, t and $X_L(t)$, we write

$$M_L \frac{d^2 X_L}{dt^2} + K_L(X_L - L/2) + \eta_L \frac{dX_L}{dt} = 0$$

which has the solution $X_L - L/2 \sim e^{\alpha t}$ with

$$\alpha = -\frac{\eta_L}{2M_L} \pm i \sqrt{\frac{K_L}{M_L}} \left[1 - \frac{\eta_L^2}{4 K_L M_L} \right]^{1/2}$$

This yields, to the lowest order in $\eta_L^2/4 K_L M_L$, remembering that $M_L = 2L^2$ and that $\omega = 2\pi/\tau_{\text{per}}$, with $\tau_{\text{per}} = t_{\text{per}}/L \approx 1.63$, $K_L \approx 8\pi^2/\tau_{\text{per}}^2$, i.e., the effective "restoring force" K_L is independent of L. On the other hand, the damping coefficient is $\eta_L = 4L\lambda_L$, were λ_L was found experimentally to decrease as $\lambda_L \sim L^{-\gamma}$ with $\gamma = 1.3$, see Section 4. Hence $\eta_L \sim L^{1-\gamma} = O(L^{-0.3})$, i.e., the damping gets weaker as $L \to \infty$.

7. DISCUSSION

We have presented here numerical results concerning the time evolution of a system with many degrees of freedom (up to 27×10^6) one of which, the position of the piston, plays a very special role. Starting with the particular initial particle distribution given by (3.1) we found two striking features of the evolution: (1) the velocity distribution of the particles approaches a Maxwellian, i.e., the system goes toward thermal equilibrium and (2) the time evolution of the piston followed closely, after some initial period, that of a damped harmonic oscillator over an extended time interval, with initial oscillations as large as $1/10$ of the system size.

As already noted, we expect from general considerations[9] that (1) should be true for any initial density $p(x, v)$ provided the number of particles N ($\sim L^3$) is large enough and one waits long enough. But what about (2)? Clearly, if we choose for $p(|v|)$ a Maxwellian, we expect only thermal fluctuations of order $O(L^{-3/2})$ in the position of the piston. This is indeed what we found numerically. For other, non-maxwellian, initial densities the question turns out to be far from trivial. We are currently working with more general initial densities and will report results in a separate paper.[19] Below we outline our program and mention some preliminary findings.

For simplicity, we assume that $p(x, v) = p(|v|)$ and $X(0) = L/2$, $V(0) = 0$. In this case there is no apriori bias for the piston to move at all, and as already noted, the hydrodynamical (deterministic) equations, see ref. 8, predict that, in the limit $L \to \infty$, the system would remain frozen in the initial state: $Y(\tau) \equiv Y(0) = 0.5$ and $W(\tau) \equiv W(0) = 0$ for all $\tau > 0$ (in the variables y and τ, see Section 2). The density $p(y, v, t)$ will also remain constant in time. But what about the particle system with a large but finite L? How will the piston and the gas behave while the particle velocities make their way to a Maxwellian?

To answer this question we note that since the initial configuration of particles is generated randomly from a Poisson process with the density $p(y, v, 0) = p(|v|)$, the actual (empirical) density of the particles, such as the one shown on Fig. 6 at $\tau = 0$, does not exactly coincide with $p(y, v, 0)$. Random fluctuations of the empirical density are typically of order $O(1/L)$. Hence, the actual initial distribution of particles can be thought of as a small perturbation of the function $p(|v|)$ and can be written as $p(|v|) + \varepsilon p_1(y, v)$ with $\varepsilon = 1/L$ and some (random) function $p_1(y, v)$ of order one.

Now, we conjecture that for large L the evolution of the particle system closely follows the solutions of the hydrodynamical equations derived in refs. 7 and 8 with a perturbed initial density $p(|v|) + \varepsilon p_1(y, v)$, rather than the stationary solution corresponding to the unperturbed density $p(|v|)$. In particular, if the latter solution is unstable, then small perturbations grow exponentially in time (in the units of $\tau = t/L$, of course), hence the system can be destabilized in $\tau \sim -\log \varepsilon = \log L$ units of time. This would be in agreement with our analysis and numerical estimates in the end of Section 4. Hence, the instability of the hydrodynamical equations becomes a key issue.

When we were finishing the present paper, we received a message from E. Caglioti and E. Presutti who (a) proved that the hydrodynamical equations are stable when $p(|v|)$ is monotonically nonincreasing in $|v|$, i.e., $p'(|v|) \leqslant 0$, and (b) suggested that they might be unstable for our class on non-monotone $p(|v|)$. We checked the suggestion (b) for our particular

density (3.1) and found that it was indeed correct; we proved that small perturbations grow exponentially in τ. Furthermore, when starting with a perturbed initial density with $\varepsilon = 0.01$, we found numerically that the corresponding solution of the hydrodynamical equations resembled very well the evolution of the particle system described here, including large nearly harmonic oscillations of the piston during the interval $10 < \tau < 30$. Further work in this direction is currently under way.[19]

Conversely, when we simulated a particle dynamics with a nonincreasing initial density $p(|v|)$ the oscillations essentially disappeared.[9] On the other hand, the particle velocity distribution still approached a Maxwellian, albeit at a somewhat slower pace.

ACKNOWLEDGMENTS

REFERENCES

1. E. Lieb, Some problems in statistical mechanics that I would like to see solved, *Phys. A* **263**:491–499 (1999).
2. Ch. Gruber, Thermodynamics of systems with internal adiabatic constraints: Time evolution of the adiabatic piston, *Eur. J. Phys.* **20**:259–266 (1999).
3. E. Kestemont, C. Van den Broeck, and M. Mansour, The "adiabatic" piston: And yet it moves, *Europhys. Lett.* **49**:143–149 (2000).
4. J. L. Lebowitz, Stationary nonequilibrium Gibbsian ensembles, *Phys. Rev.* **114**:1192–1202 (1959).
5. Ch. Gruber and L. Frachebourg, On the adiabatic properties of a stochastic adiabatic wall: Evolution, stationary non-equilibrium, and equilibrium states, *Phys. A* **272**:392–428 (1999).
6. Ch. Gruber and J. Piasecki, Stationary motion of the adiabatic piston, *Phys. A* **268**:412–423 (1999).
7. J. L. Lebowitz, J. Piasecki, and Ya. Sinai, Scaling dynamics of a massive piston in an ideal gas, in *Hard Ball Systems and the Lorentz Gas*, Encycl. Math. Sci., Vol. 101 (Springer, Berlin, 2000), pp. 217–227.
8. N. Chernov, J. L. Lebowitz, and Ya. Sinai, *Scaling Dynamic of a Massive Piston in a Cube Filled With Ideal Gas: Exact Results*, this volume of the journal.

---

[9] We tried a uniform "flat" function given by $p(|v|) = 1$ for $|v| \leqslant v_{max}$ and a triangular one $p(|v|) = 1 - |v|/v_{max}$.

9. L. Boltzmann, Reply to Zermelo's remarks on the theory of heat, *Annalen der Physik* **57**:773 (1896); reprinted and translated as Chapter 8 in S. G. Brush: *Kinetic Theory* (Pergamon, Oxford, 1966).

10. J. L. Lebowitz, Macroscopic laws and microscopic dynamics, time's arrow and Boltzmann's entropy, *Phys. A* **194**:1–27 (1994).

11. M. Matsumoto and T. Nishimura, Mersenne Twister: A 623-dimensionally equidistributed uniform pseudorandom number generator, *ACM Trans. Model. Comp. Simul.* **8**:3–30 (1998).

12. R. Holley, The motion of a heavy particle in an infinite one dimensional gas of hard spheres, *Z. Wahrschein. verw. Geb.* **17**:181–219 (1971).

13. D. Dürr, S. Goldstein, and J. L. Lebowitz, A mechanical model of Brownian motion, *Commun. Math. Phys.* **78**:507–530 (1981).

14. R. Lupton, *Statistics in Theory and Practice* (Princeton University Press, Princeton, NJ, 1993).

15. I. P. Cornfeld, S. V. Fomin, and Ya. G. Sinai, *Ergodic Theory*, Fundamental Principles of Mathematical Sciences, Vol. 245 (Springer-Verlag, New York, 1982).

16. N. Chernov, Entropy, Lyapunov exponents and mean-free path for billiards, *J. Statist. Phys.* **88**:1–29 (1997).

17. S. Kerckhoff, H. Masur, and J. Smillie, Ergodicity of billiard flows and quadratic differentials, *Ann. of Math.* **124**:293–311 (1986).

18. Ch. Gruber, S. Pache, and A. Lesne, *Deterministic motion of the controversial piston in the thermodynamic limit*, manuscript.

19. E. Caglioti, N. Chernov, J. L. Lebowitz, and E. Presutti, in preparation.

20. Ya. B. Vorobets, Ergodicity of billiards in polygons: Explicit examples, *Uspekhi Mat. Nauk* **51**:151–152 (1996).